

Introducing hydrophilic carbon nanoparticles into hydrophilic sol-gel film electrodes

Stuart M. Macdonald · Katarzyna Szot ·
Joanna Niedziolka · Frank Marken · Marcin Opallo

Received: 25 May 2007 / Revised: 6 July 2007 / Accepted: 10 July 2007 / Published online: 11 August 2007
© Springer-Verlag 2007

Abstract A hydrophilic carbon nanoparticle–sol-gel electrode with good electrical conductivity within the sol-gel matrix is prepared. Sulfonated carbon nanoparticles with high hydrophilicity and of 10–20 nm diameter (Emperor 2000) are co-deposited onto tin-doped indium oxide substrates employing a sol-gel technique. The resulting carbon nanoparticle-sol-gel composite electrodes are characterized as a function of composition and salt (KCl) additive. Scanning electron microscopy and voltammetry in the absence and in the presence of a solution redox system suggest that the composite electrode films can be made electrically conducting and highly porous to promote electron transport and transfer. The effect of the presence of hydrophilic carbon nanoparticles is explored for the following processes: (1) double layer charging, (2) diffusion and adsorption of the electrochemically reversible solution redox system 1,1'-ferrocenedimethanol, (3) electron transfer to the electrochemically irreversible redox system hydrogen peroxide, and (4) electron transfer to the redox liquid tert-butylferrocene deposited into the porous composite electrode film. The extended electrochemically active hydrophilic surface area is beneficial in particular for surface sensitive processes (1) and (3), and it provides an extended solid|organic liquid|aqueous solution boundary for reaction (4).

The carbon nanoparticle–sol-gel composite electrodes are optimized to provide good electrical conductivity and to remain stable during electrochemical investigation.

Keywords Carbon nanoparticle sol-gel · Thin film · Hydrogen peroxide · Redox liquid · Sensor · Voltammetry

Introduction

The characteristics and performance of electrodes made of carbon-based materials are strongly dependent on the chemical and physical properties resulting from particular carbon and composite structures [1, 2]. In particular, the immobilization of carbon-based nanomaterials, such as carbon nanoparticles (CNPs), nanotubes, or carbon nanofibers, allows tailored electrode surface properties to be achieved, e.g., with respect to the type of reactive sites or the mode of reactant transport towards the electrode surface. Diffusion effects in porous carbons [3], the enhancement of electrocatalytic properties [2, 4], stable enzyme immobilization [5, 6], liquid immobilization [7, 8], or high efficiency of triple phase boundary electrode processes [7] at carbon electrodes have been reported on specific carbon structures.

CNPs (or carbon blacks) represent a very interesting well-known carbon material, which offers all the advantages of nanocarbons (extremely high surface area, adsorption sites, reactive surface sites, conductivity, etc.). They are particulate forms of highly dispersed elemental carbon and manufactured for example by controlled vapor-phase pyrolysis of hydrocarbons [9]. In this study, a special hydrophilic type of CNPs with surface immobilized phenyl-sulfonic acid groups (Emperor 2000, Cabot) is employed.

S. M. Macdonald · F. Marken
Department of Chemistry, University of Bath,
Bath BA2 7AY, UK

K. Szot · J. Niedziolka · M. Opallo (✉)
Institute of Physical Chemistry, Polish Academy of Sciences,
ul. Kasprzaka 44/52,
01-224 Warszawa, Poland
e-mail: mopallo@ichf.edu.pl

The immobilization of CNPs as an active thin film on the electrode surfaces is affected by the dispersion and particle aggregation. In the present work, the sol-gel process was employed for the deposition of stable CNP-sol-gel composite films at electrode surfaces. In earlier studies, various silica based electrically conductive composite bulk materials were obtained with carbon blacks [10–12], and these were used for example as gas diffusion electrodes in solid state electrochemical cells [13, 14] or as supercapacitors [15].

The carbon encapsulation into sol-gel silicate thin films was also proposed for the stable immobilization of carbon nanotubes [3] and carbon nanofibers [7, 16] at electrode surfaces. These electrodes were examined in aqueous solutions, and they are of interest for a range of important applications (sensors, supercapacitors, active membranes, etc.). The benefits of immobilizing of carbon microparticles (typically 20 μm diameter) into a silicate matrix were reported first by Lev's group [17, 18]. It is highly interesting to extend this work to even smaller particles, which would provide several orders of magnitude higher surface area [18, 19]. An attempt to achieve an extremely high active surface area with very small hydrophilic CNPs is made in this study. A key problem in the work with small hydrophilic nanoparticles (which are negatively charged and which need to be embedded into a negatively charged silica matrix) is achieving sufficient electrical conductivity through the resulting composite film, and this is addressed here with a method based on colloid destabilization via salt addition. Alternative method of immobilization of CNPs on the electrode surface based on layer by layer electrostatic deposition with cationic polymer was also recently reported [20].

In this work CNP-sol-gel thin film electrodes are prepared by sol drop deposition of a mixture of a tetramethoxysilane with a CNP dispersion in aqueous solution in the presence of added salt. To optimize the electrode properties and the CNP aggregation, the starting sol composition was adjusted by changing the CNP amount and the salt (KCl) concentration. The new electrodes were examined by scanning electron microscopy (SEM) and cyclic voltammetry. To investigate the effect of the CNP content on electrode processes, several test systems have been chosen: (1) double layer charging, (2) solution phase processes with reversible and irreversible heterogeneous electron transfer, and (3) the heterogeneous three-phase junction electrochemical oxidation of tert-butylferrocene. It is shown that results obtained with CNP-sol-gel film electrodes compare favorably with results from earlier experiments with nanoparticulate, nanoporous, or microporous materials [7, 8, 21–28]. Further applications of the highly active hydrophilic carbon nanoparticle-sol-gel composite electrode are proposed.

Experimental

Chemical reagents

Emperor 2000 CNPs (about 9 to 18 nm diameter, Emperor 2000, Cabot) is a fluffy pigment black, with phenylsulfonic acid surface functionalities, easily dispersed in aqueous solution, with a typical bulk density of 320 g dm^{-3} . Tin-doped indium oxide (ITO, typically 15Ω per square) coated glass electrodes were obtained from Image Optics, Basildon, UK.

Tetramethoxyorthosilicate (TMOS; 99%), and tert-butylferrocene (tBuFc, 98%) were obtained from ABCR. Hydrogen peroxide and 1,1'-ferrocenedimethanol [Fc (CH_2OH)₂] were purchased from Aldrich. NaClO_4 and KCl (analytical grade) were obtained from POCh. All chemicals were used as received. Water was filtered and cleansed using an ELIX system (Millipore, resistivity $>18 \text{ M}\Omega \text{ cm}$). All experiments were conducted at $20 \pm 2 \text{ }^\circ\text{C}$.

Electrode preparation

Before use, the ITO electrodes were cleaned with water and ethanol. A working area on each electrode of 0.2 cm^2 was marked out using Scotch Magic Tape (3M). Next, the active area was modified by deposition of a 20 μl volume of a mixture of 1 μl freshly prepared sol (a) and 100 μl carbon nanoparticle suspension (b). The sol (a) was prepared by mixing 0.5 cm^3 TMOS with 0.125 cm^3 water. Subsequent addition of 27.5 μl 0.04 mol dm^{-3} HCl initiated the sol-gel process. The mixture was then sonicated for 10 min. The carbon nanoparticle suspension (b) consisted typically of 0.025 g of Emperor 2000 CNPs dispersed in 10 cm^3 aqueous KCl solution (typically 50 mM KCl, see text). Next, sol (a) and carbon nanoparticle suspension (b) were mixed in a sol/suspension ratio of 1:100. The mixture was then sonicated for a further 10 min before being deposited by pipette onto the ITO electrode. After evaporation of water and methanol and 24 h gelation, the film deposit consists of approximately 0.3 mg silicate and 0.25 mg CNPs (45 wt% CNPs).

For the modification of the carbon nanoparticle-sol-gel electrode with tert-butylferrocene, a solvent evaporation method was employed. A solution of 5 μl tBuFc solution in hexane (1:1,000 v/v ratio) was prepared and 10 μl of this deposited onto the film electrode. After evaporation of the hexane, about 40 nmol tBuFc was immobilized into the porous carbon nanoparticle-sol-gel electrode.

Instrumentation

SEM images were obtained with a JEOL JSM6310 or with a Leo 1530 field emission gun scanning electron microscope

system. Cyclic voltammograms were recorded with an Autolab PGSTAT30 (Eco Chemie, Netherlands) electrochemical analyzer in a conventional three-electrode electrochemical cell. A Ag|AgCl(saturated KCl) and platinum wire were used as reference and counter electrodes, respectively.

Results and discussion

Formation of carbon nanoparticle–sol-gel electrodes and double layer charging effects

Thin film carbon nanoparticle–sol-gel electrodes were deposited onto tin-doped indium oxide (ITO) surfaces in a solvent evaporation process (see [experimental](#)). An initial electrochemical characterization was conducted in aqueous 0.1 M NaClO₄. The presence of the CNPs is immediately revealed by the substantial capacitive charging current (see Fig. 1). Similar capacitive current effects were reported earlier for example for electrodes modified with carbon nanoparticle–poly(diallyl-dimethylammoniumchloride) [20] or carbon nanofiber–sol-gel films [7].

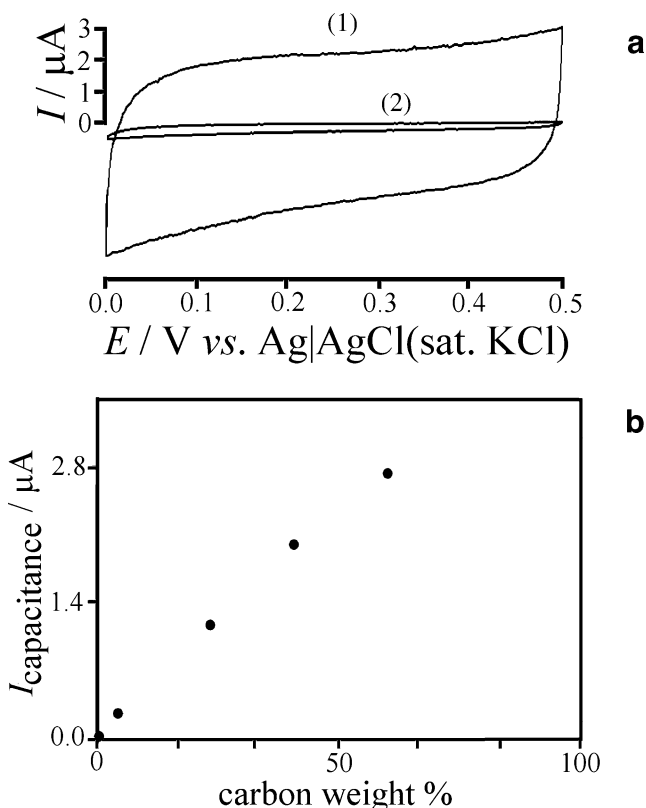


Fig. 1 **a** Cyclic voltammograms (scan rate 10 mV s⁻¹) obtained in 0.1 mol dm⁻³ aqueous NaClO₄ for CNP–sol-gel film electrodes with (1) 45 wt% and (2) 4.5 wt% carbon nanoparticles (prepared using 50 mM KCl aq). **b** Plot of the capacitive current response vs the carbon weight percent in the CNP–sol-gel film electrode

Unsurprisingly, the capacitive current for a 45 wt% carbon nanoparticle deposit (curve 1) is considerably larger compared to that obtained with a 4.5 wt% deposit (curve 2) or that obtained at bare ITO electrodes (not shown). The substantial increase in capacitive background current demonstrates good electrical conductivity throughout the film deposit. A plot of the capacitive current vs the carbon nanoparticle content in film deposits shows a good correlation, although at carbon nanoparticle contents of more than 50 to 60 wt%, film electrodes became mechanically unstable during immersion and removal from solution. For the 45 wt% carbon nanoparticle electrode (with 0.25 mg CNPs) a specific capacitance of 0.8 Fg⁻¹ can be calculated. This value seems low when compared to other carbon materials [29], but this is believed to be due to a shielding effect in carbon aggregates. For the immobilized carbon in the CNP–sol-gel film, the observed capacitance corresponds approximately to an active surface area (assuming 10 μFcm⁻² [30]) of about 10 m² g⁻¹. This compares to a calculated surface area of typically 100 m² g⁻¹ (calculated assuming 20 nm diameter particles) suggesting that approximately 10% of the total carbon surface is active. A substantial part of the apparently inactive surface may be contained within carbon aggregates.

SEM images for the carbon nanoparticle material (a) and for the carbon nanoparticle–sol-gel film electrodes (b, c) are shown in Fig. 2. Aggregates of CNPs several microns in diameter are heterogeneously distributed in the composite film. It is likely that they provide percolation paths for electrical conductivity through the film.

Voltammetry with a reversible solution phase redox system: oxidation of 1,1'-ferrocenedimethanol

Next, a reversible one electron solution phase redox system was studied. The electro-oxidation of Fc(CH₂OH)₂ was investigated in aqueous 0.1 M NaClO₄ (Eq. 1).

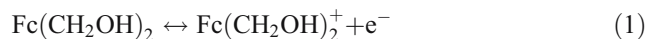


Figure 3a compares voltammograms obtained in a 1 M Fc(CH₂OH)₂ solution with (1) a 45 wt% CNP electrode, (2) a bare ITO electrode, and (3) a 0 wt% CNP electrode (only sol-gel film). For the silicate-coated electrode (3) the reduced mobility of 1,1'-ferrocenedimethanol within the gel film is clearly observed. The anodic peak current observed at the 45 wt% CNP–sol-gel electrode (1) is approximately twice comparing to that obtained at a bare ITO electrode (2). In addition to facile electron transfer at the CNP–sol-gel film, trapping of solution within the porous carbon structure occurs. A more symmetric voltammetric peak system similar to that anticipated for the case of trapping of Fc(CH₂OH)₂ containing solution within the

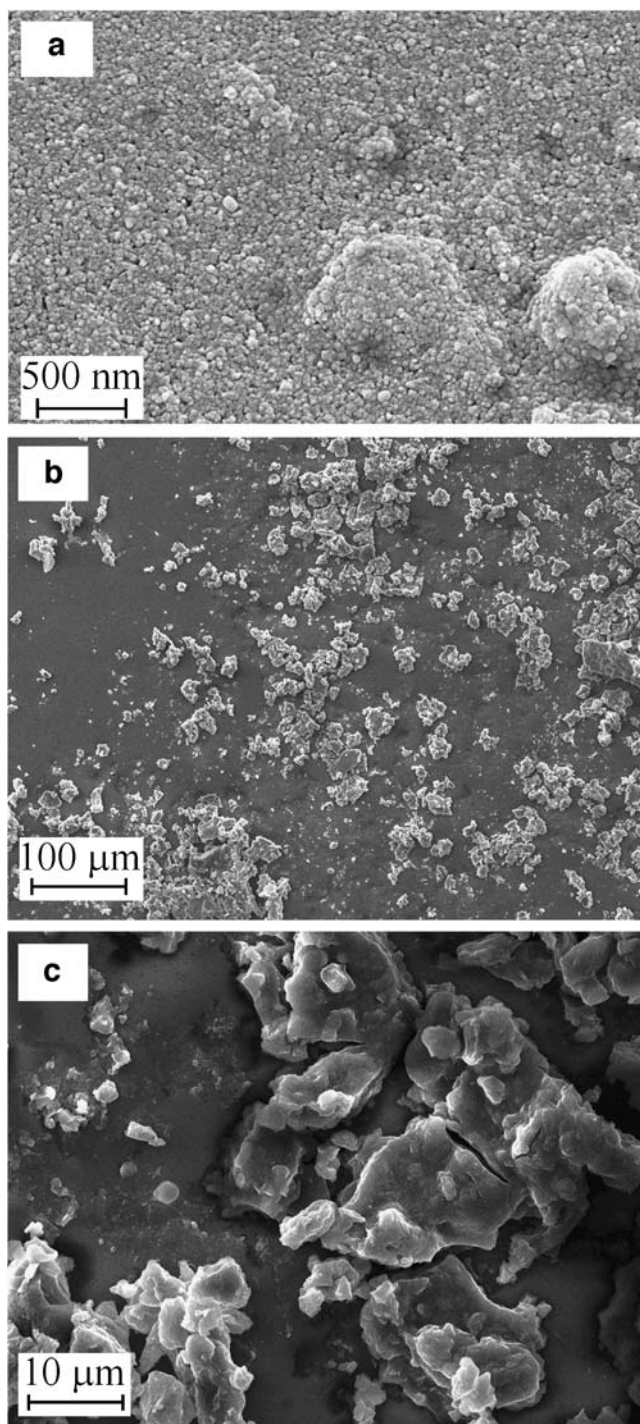


Fig. 2 Typical SEM images of the surface of hydrophilic carbon nanoparticle–sol-gel film deposits on ITO substrates: **a** Only carbon nanoparticles deposited from an aqueous dispersion; **b** low magnification image of the CNP–sol-gel film; **c** high magnification of the CNP–sol-gel film. The films in (**b**, **c**) were obtained from 45 wt% of CNP (prepared using 50 mM KCl) in sol-gel matrix

carbon is observed. The plot of the anodic peak current vs the carbon nanoparticle weight percent content reveals the increase of the peak current probably due to a trapped volume of liquid (see Fig. 3b). The decrease of the anodic

peak current at higher carbon loadings is believed to be due to the mechanical deterioration of the more brittle films with high carbon content.

The behaviour of the porous CNP–sol-gel electrodes in the presence of an electrochemically reversible solution redox system is dominated in approximately equal amounts by diffusion toward the outer electrode surface and trapped solution within the pores. Similar effects of porous deposits on simple redox processes were observed for electrodes modified with ITO nanoparticles deposits [21] or micropo-

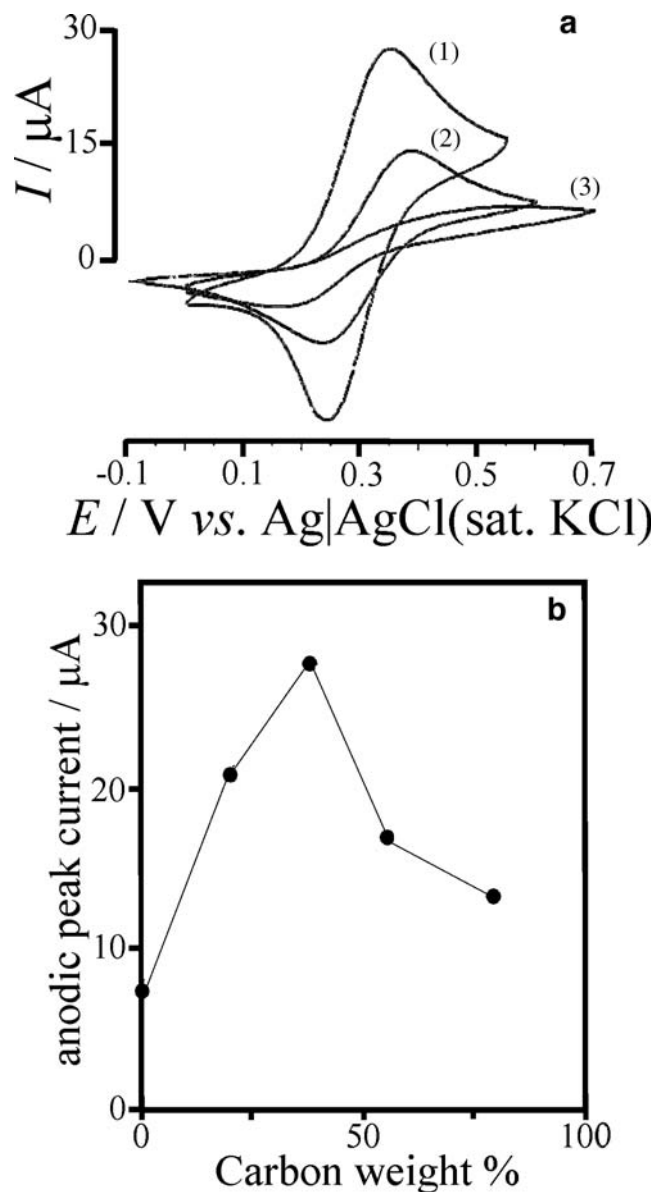


Fig. 3 a Cyclic voltammograms (scan rate 10 mV s^{-1}) for the oxidation of 1 mM 1,1'-ferrocenedimethanol in aqueous 0.1 M NaClO_4 obtained with (1) a carbon nanoparticle–sol-gel electrode (45 wt% CNP, 50 mM KCl), (2) a bare ITO electrode, and (3) 0 wt% CNP–sol-gel film electrode. **b** Plot of the anodic peak current vs the carbon nanoparticle content in the CNP–sol-gel film electrode

rous layers of gold [22] or three dimensional ultramicroelectrode ensembles [23].

To optimize the electrode formation process, KCl was added to the mixture of sol-gel and carbon nanoparticle suspension (see “Experimental”). During evaporation of water and methanol and gelation, KCl enrichment causes changes in the carbon nanoparticle aggregation and the resulting in modified composite film structures. Although mechanistic details for this effect are not known, the systematic increase in the anodic current peak for the 1,1'-ferrocenedimethanol oxidation from the diffusion controlled level (at 0 mM KCl) to a considerably increased current (at 50 mM KCl) is clearly observed (see Fig. 4). The KCl is believed to interact with the carbon aggregates to produce a more accessible and conducting carbon structure. The salt concentration of 50 mM KCl was most

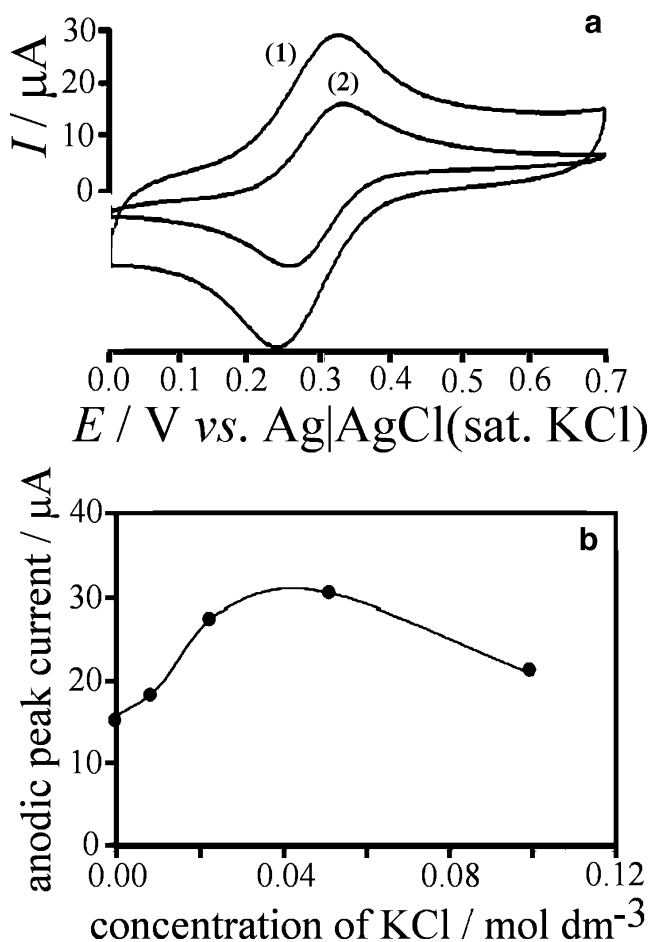


Fig. 4 **a** Cyclic voltammograms (scan rate 10 mV s^{-1}) for the oxidation of 1 mM 1,1'-ferrocenedimethanol in aqueous 0.1 M NaClO_4 obtained with a CNP-sol-gel film electrode with 45 wt\% CNPs. The salt (KCl) content of the deposition solution was varied during the film formation and cyclic voltammograms are shown for (1) no KCl added and (2) 50 mM KCl added (see “Experimental”). **b** Plot of the anodic peak current vs the KCl concentration in the deposition solution

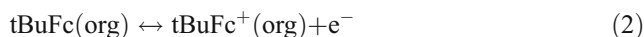
beneficial and therefore employed for most of the following experiments.

Voltammetry with an irreversible solution phase redox system: reduction of hydrogen peroxide

The examination of the presence of CNPs on the electrochemically highly irreversible reduction of hydrogen peroxide revealed an approximately 20-fold increase of the faradic current for the H_2O_2 reduction (see Fig. 5). The current is further increased with higher carbon loading (see Fig. 4b). Previously, a catalytic effect of immobilized carbon nanotubes on the hydrogen peroxide electrooxidation was reported [31]. However, in this study, only the enhanced reduction is observed probably predominantly caused by the extremely high surface area and of the CNPs and specific geometry of diffusional space. The effect of surface area is confirmed by similar signal-to-noise ratio (calculated as ratio of the current at 0.1 V to that at 0.55 V) equal approximately 10. This effect is more important for slow heterogeneous electron transfer reactions as has been observed earlier for example for electrodes containing microporous layers of gold [22] or at three dimensional ultramicroelectrode ensembles [23].

Voltammetry with a deposited redox liquid: oxidation of tert-butylferrocene

Next, preliminary experiments with the redox liquid tert-butylferrocene were conducted. The water insoluble liquid was deposited into porous electrode (see “Experimental”). In this voltammetric experiment, a peak-shaped response is expected to be associated with the oxidation of tBuFc to tBuFc⁺ (Eq. 2).



At a bare ITO electrode, this process is highly ineffective (see Fig. 6, curve 4) due to the formation of extended droplets which block the electrode surface. However, in the porous structure of the CNP-sol-gel electrode the tBuFc liquid is dispersed, and the oxidation can proceed at an extended triple-phase boundary [7, 25]. Figure 6 shows data for three consecutive potential cycles recorded for a 40 nmol tBuFc deposit. The charge under the oxidation peak, approximately $600 \mu\text{C}$, is consistent with about 6 nmol electrons being transferred (or 15% of tBuFc deposit is converted). This behavior of the electrode is related to the development of largely extended three-phase junctions CNP|tert.-butylferrocene|aqueous electrolyte interface [7, 21, 25]. The efficiency of reaction (2) is similar to obtained with tBuFc deposit present on Au covered hydrophobic silicate

film [24] and carbon nanofibers [7] or ITO nanoparticles embedded in hydrophobic silicate film [21].

The CNP–sol-gel electrode film appears to be wetted by the hydrophobic redox liquid tBuFc, and it retains its electrochemical activity even after several potential cycles. A slow decrease of the voltammetric response can be explained with the slow loss of some oxidized material into the solution phase (Eq. 3).



This reaction occurs to maintain charge neutrality of organic deposit. The second competing reaction, the transfer of a counter anion from the aqueous into the organic phase (see Eq. 4), is likely to occur simultaneously

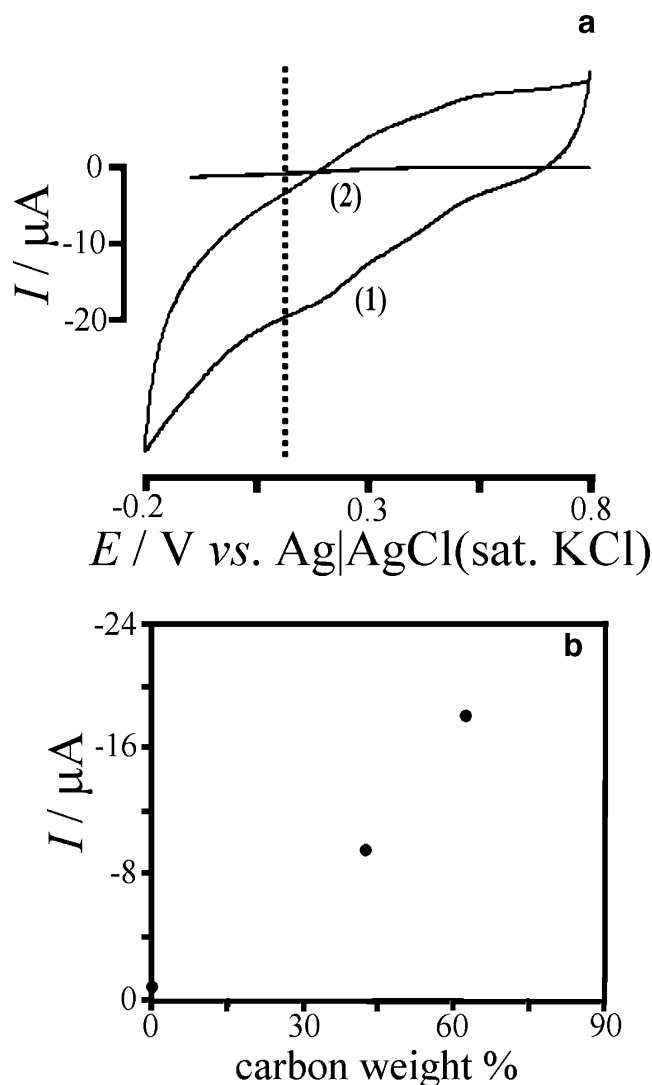


Fig. 5 **a** Cyclic voltammograms (scan rate 10 mV s^{-1}) obtained in $50 \text{ mM H}_2\text{O}_2$ solution in $0.1 \text{ M H}_2\text{SO}_4$ aq. with (1) a 45 wt% CNP–sol-gel electrode and (2) a bare ITO electrode. **b** Plot of the effect of the CNP loading on the reduction current at 0.1 V vs $\text{Ag}|\text{AgCl}(\text{sat. KCl})$

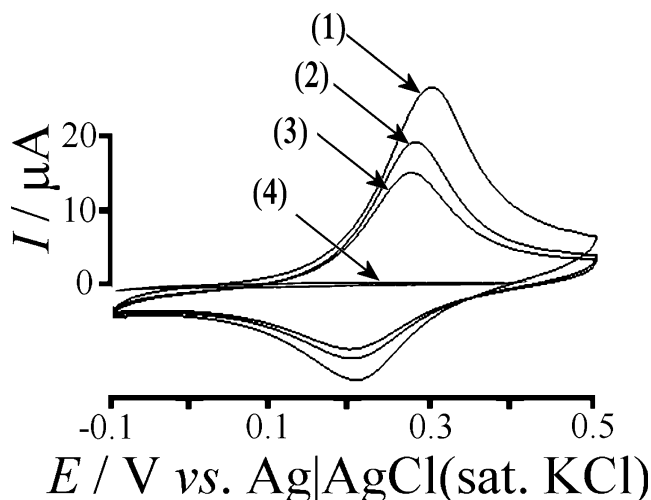
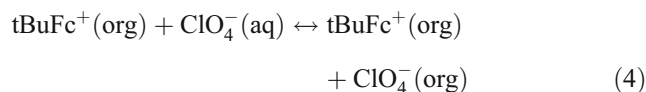


Fig. 6 Cyclic voltammograms (scan rate 10 mV s^{-1}) for the oxidation of tert-butylferrocene (40 nmol) immobilized at a 45 wt% carbon nanoparticle–sol-gel film electrode (50 mM KCl) immersed in aqueous 0.1 M NaClO_4 : in (1–3) are potential cycles 1 to 3 are shown; (4) cyclic voltammogram obtained under the same conditions at a bare ITO electrode

and would provide anion selectivity for example in sensor applications.



Porous high surface area electrodes are very useful, and the incorporation of CNPs in sol-gel silicas is an effective way to combine functionality (e.g., introduced by functionalized sol-gel precursors) with high active surface area and conductivity. Further optimization of this type of electrode and applications in sensing or energy storage are possible.

Conclusions

A porous electrode modified with hydrophilic CNPs was prepared from a suspension using a sol-gel methodology and drop deposition. The CNPs form micrometer-sized aggregates in the presence of added salt, and their presence in the hydrophilic silicate film substantially extends the electrochemically active surface. The double layer capacitance is substantially increased. The effect of the electrode on reversible solution phase redox systems is consistent with other high surface area electrodes. For kinetically slow electrode reactions (such as the hydrogen peroxide electroreduction), the magnitude of the current dramatically increases with carbon nanoparticle content due to the increase of reactive surface area. Similarly, a dramatic effect is observed for three-phase junction electrode processes (which suppress capacitive background currents) such as the oxidation of the redox liquid deposit of tert-butylferrocene.

Acknowledgements The support from the Royal Society (project “Novel ion transfer electrodes and ion transfer processes”) and from the Ministry of Science and Higher Education of Poland (research project 3 T09A 019 26) is gratefully acknowledged. We thank Cabot for generous support with carbon nanoparticle materials.

References

1. Mc Creery RL (1990) In: Bard AJ (ed) *Electroanalytical chemistry*, vol. 17. Marcel Dekker, New York, p 221
2. Banks CE, Davies TJ, Wildgoose GG, Compton RG (2005) *Chem Commun* 7:829
3. Gong K, Zhang M, Yan Y, Su L, Mao L, Xiong S, Chen Y (2004) *Anal Chem* 76:6500
4. Dai X, Wildgoose GG, Compton RG (2006) *Analyst* 131:1241
5. Ghanem MA, Marken F (2005) *Electrochem Commun* 7:1333
6. Zhang M, Smith A, Gorski W (2004) *Anal Chem* 76:5045
7. Niedziolka J, Murphy MA, Marken F, Opallo M (2006) *Electrochim Acta* 51:5897
8. Zhao F, Wu XE, Wang MK, Liu Y, Gao LX, Dong SJ (2004) *Anal Chem* 76:4960
9. Dannenberg EM, Paquin L, Gwinnell H (1992) *Encyclopedia of chemical technology*, vol. 4. 4th edn. Wiley, New York, p 1037
10. Fujiki K, Ogasawara T, Tsubokawa N (1998) *J Mater Sci* 33:1871
11. Hubert T, Shimamura A, Klyszcz A (2004) *J Sol-Gel Sci Technol* 32:131
12. Hubert T, Shimamura A, Klyszcz A (2005) *Mater Sci (Poland)* 23:61
13. Nishikawa O, Doyama K, Miyatake K, Uchida H, Watanabe M (2004) *Electrochemistry* 72:232
14. Nishikawa O, Doyama K, Miyatake K, Uchida H, Watanabe M (2005) *Electrochim Acta* 50:2719
15. Min M, Machida K, Jang HJ, Naoi K (2006) *J Electrochem Soc* 153:A334
16. Rozniecka E, Niedziolka J, Murphy MA, Sirieix-Plenet J, Gaillon L, Marken F, Opallo M (2006) *J Electroanal Chem* 587:133
17. Tsionsky M, Gun G, Glezer V, Lev O (1994) *Anal Chem* 66:1747
18. Rabinovich L, Lev O (2001) *Electroanalysis* 13:265
19. Sampath S, Lev O (1996) *Anal Chem* 68:2015
20. Amiri M, Shahrokhian S, Marken F (2007) *Electroanalysis* 19:1032
21. Niedziolka J, Szot K, Marken F, Opallo M (2007) *Electroanalysis* 19:155
22. Szamocki R, Reculosa S, Ravaine S, Bartlett PN, Kuhn A, Hempelmann R (2006) *Angew Chem Int Ed* 45:1317
23. De Leo M, Kuhn A, Ugo P (2007) *Electroanalysis* 19:227
24. Niedziolka J, Opallo M (2004) *Electrochem Commun* 6:475
25. McKenzie KJ, Niedziolka J, Paddon CA, Marken F, Rozniecka E, Opallo M (2004) *Analyst* 129:1181
26. Katz E, Willner I (2004) *ChemPhysChem* 5:1084
27. Milsom EV, Novak J, Oyama M, Marken F (2007) *Electrochem Commun* 9:436
28. Milsom EV, Perrott HR, Peter LM, Marken F (2005) *Langmuir* 21:9482
29. Marken F, Gerrard ML, Mellor IM, Mortimer RJ, Madden CE, Fletcher S, Holt K, Foord JS, Dahm RH, Page F (2001) *Electrochem Commun* 3:177
30. Zoltowski P (1976/77) *J Power Sources* 1:285
31. Wang J, Musameh M, Lin Y (2003) *J Am Chem Soc* 125:2408